Applying Electromagnetic Field Analysis to Minimize the Earth Resistance on High Resistivity Soils

Silvia Ronda*, **Clara Oliver, Oibar Martinez, Patricia Marquez, and Jose M. Miranda**

Abstract—Different optimization strategies to reduce the earth resistance in a high resistivity soil are discussed in this work and illustrated with a practical example. Finite Element simulations reproducing real-world conditions in terms of structure design and soil profiles have been made to evaluate the improvements that should be adopted to minimize earth resistance. We analyze an example of an earthing system of an array of four identical telescopes installed on high resistivity (kΩ· m order) soils with two different behaviors. In the first one, current dissipation occurs in an uniform soil. In the second one, a terrain with four layers of different resistivities is considered. This situation corresponds to a real world case of an observatory constructed in a volcanic terrain. It was found that the best strategy in each case differs: extend horizontal electrodes as far as possible from the foundation in the first case and combine these electrodes with buried vertical electrodes that connect with deep high conductive layers in the second. The results are discussed in terms of the achieved improvements depending on the modifications introduced in the main structure.

1. LOWERING THE EARTH RESISTANCE: MOTIVATION AND OVERVIEW

The earth electrical resistance plays a major role in the safety of both personnel and instrumentation. Grounding is also a fundamental part of any lightning protection system. It is vitally important, as explained in the standards related to lightning protection [1–4] that in the event of a lightning strike, excess charge induced in the lightning rods finds a safe and low resistance path to follow for its correct dissipation in order to prevent any damage. Moreover, a high earth resistance may compromise the proper operation of the surge protection devices. It is therefore understandable that a number of standards that regulate the implementation of grounding are within the framework of protection against atmospheric discharges.

Local regulations not always pose specific limits to a maximum acceptable earth resistance. This is the case of the *Low Voltage Electrotechnical Regulation.* For this standard, the maximum earth resistance will be the one which ensures that, throughout the life of the installation and at any time of the year, touch voltages greater than 24 V cannot be produced in the accessible metal parts of the installation, being 50 V for the rest of the parts [5]. But even in these cases one should note that touch and step voltages are better controlled with low earth resistances.

European standards such as EN-62305-3 [3] recommend specific limits to earth resistance, less than 10 Ω when being measured at low frequency. However, in EN-62305-3 it is also mentioned that the recommended value of the global earth resistance of 10 Ω is quite conservative in the case of structures in which direct equipotential bonding is applied. It also remarks that, although the value of resistance must be as low as possible in all cases, the most important measure is the equipotential bonding.

The standard improvements which can be made to reduce the earth resistance in difficult terrains are generally based on:

a) burying horizontal conductive plates or meshes,

b) burying vertical electrodes connected in parallel or

c) modifying the own terrain, which can be done by either changing the entire terrain material in a large volume or adding earthing enhancing compounds.

A combination of several procedures is also possible. For instance, the Taiwan Photon Source (TPS) storage ring has a $0.2\,\Omega$ earth system with 62 vertical electrodes and a grid of 4 rings. Bentonite was used to lower the resistivity of the terrain [6]. Some theoretical models for basic configuration of vertical electrodes and horizontal grids are adopted in the standards BS 7430:2011 [7] MIL-HDBK-319A [8] and summarised in [9].

The use of vertical electrodes connected in parallel poses several practical limitations. In order to prevent loss of effectiveness, it is necessary to keep a minimum distance between electrodes, which is typically around 5 times larger than the electrode length. Otherwise, the overlapping of the local equipotential lines around each electrode reduces the efficiency of the configuration. Typical electrode lengths can be 2–3 m. The amount of resistance that is reduced with each additional electrode decreases as the number of electrodes increases, but the basic parallel resistor formula of circuit theory will always underestimate the final resistance.

It is generally accepted that the electrodes should usually be installed with a backfilling material of high conductivity, which increases the effective diameter. Concrete is hygroscopic and has a resistivity of 30–$90\,\Omega\cdot\text{m}$. This is particularly interesting in medium and highly resistive soils because a wire or metallic rod encased in concrete has lower resistance than a similar electrode buried directly in the earth. Some models of the calculation of the resistance of a grid with encased vertical electrodes can be found in the IEEE Std 80-2000 [10].

One solution could be replacing the soil with a low resistance material [11]. A number of earth enhancement materials are commercially available. Many are composed of carbon-based materials or clays like bentonite (or a mixture of both). These materials can also be used as backfilling materials to improve the resistance of an electrode. Chemical treatment of soil has environmental implications and should not be considered as a long term solution, and there is additionally a risk of corroding the earthing system. Coke breeze has also been used, but it poses serious concerns due to its highly corrosive nature. IEC 62561-7 standard discusses prequalification methods for ground enhancement materials [12].

Bentonite clay is actually a natural earth soil, mostly composed of the mineral montmorillionite, which was formed by volcanic action in the past. It is noncorrosive, stable, and has a resistivity of $2.5\,\Omega\cdot\text{m}$ at 300% moisture. It has almost no environmental concerns and will not corrode the copper like other compounds based on carbon. Bentonite is hygroscopic, but just because of this it needs moisture in the ground to maintain its properties.

Some earthing enhancement materials contain cement, which after installation acquire properties that are very close to concrete. This prevents the material from leaching into the soil or washing away by groundwater. This type of material does not require any maintenance and has been shown to significantly reduce the long-term resistance of grounding electrodes in a study commissioned by the National Fire Protection Research Foundation [13]. However, alternatives should be considered because these solutions could not be feasible in terms of environmental conservation and costs. This could be the case when earthing must be done in areas of difficult access and with soils that are hard to excavate.

2. A CASE STUDY: LST SUBARRAY OF CTA-NORTH PROJECT

In order to illustrate how the electromagnetic field analysis can help to optimize the design of an earthing system, we analyze a practical example with challenging demands: The earthing system of an array of four telescopes built in a soil of volcanic nature and very low humidity content.

Cherenkov Telescope Array (CTA) North Project aims to build a large scale observatory hosting four Large-Sized Telescopes (LST) and another subarray of smaller, Medium-Sized Telescopes (MST). CTA-North subarrays are located in the Roque de los Muchachos Observatory, a protected area with regulations that pose severe limits to land removal operations and uses of earth enhancement compounds.

2.1. Description of the Telescopes

The LST is an instrument with a mechanical structure hosting several sensitive optical and electronics subsystems. Figure 1 shows a picture of the localization of all the LST (1-4) and a photo of the first telescope built in the observatory, the LST1.
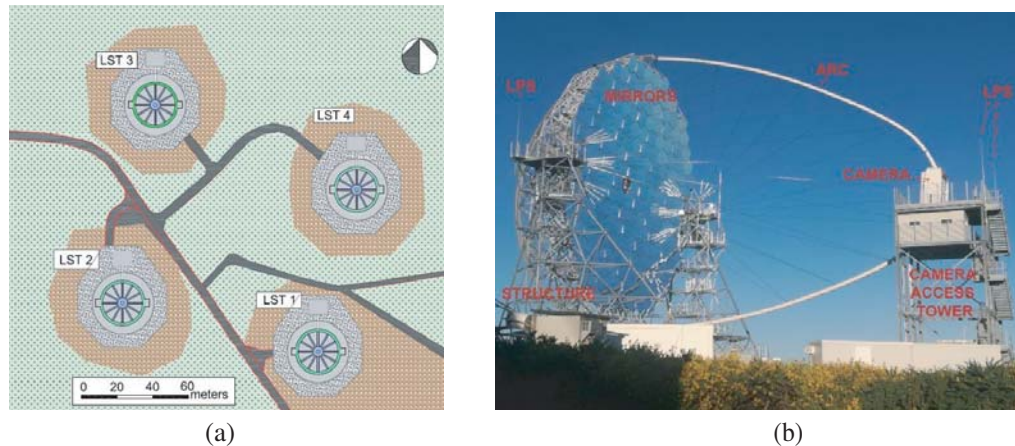

(a)   (b)

Figure 1. Current view of the localization of (a) the four LSTs and (b) photo of LST1.

LST supports an array of 198 mirror plates, which conform a parabolic dish of 23 m diameter. The mirror plates are mounted on a structure of tubes. Tubes are composed of galvanized steel, aluminium, and carbon fibre. Each mirror can be moved with two actuators. The mirrors focus the light on a camera composed by an array of fast photomultipliers and associated electronics, and the recorded data are sent via optical fibres to a control room for further processing and storage.

The camera is the most complex system of the telescope and has two input power lines: one phase 230 V UPS and 3 phases AC 400 V. Inside the camera, both lines feed the main power distribution box, which contains surge protection devices. The UPS line feeds those elements that need power for safety reasons in case of a power failure. The other one feeds the rest of the camera subsystems either directly or through 24 V power supplies.

The telescope structure rests on seven points, with the central axis of rotation and six moving bogies equally spaced in a hexagonal arrangement. The bogies run on a circular rail of 23.9 m diameter and 500 mm width, which is fixed to the terrain with a concrete foundation. The total weight of LST telescope is 103 tons [14, 15].

2.2. Soil Conductivity Surveys

During the earthing system design, soil conductivity was one of the elements that received special attention, since it has an important influence on earth resistance value [16, 17]. In practice, earth resistance is roughly inversely proportional to soil conductivity. This parameter was measured for the four telescope sites using Wenner method [18]. A significant diversity of values was found among the sites, and all of them exhibited conductivities below 1 mS/m. All sites except LST3 showed uniform conductivity up to depths of 10 m. However, in LST3 the terrain corresponds to a non-homogeneous soil with extremely low conductivity layers due the presence of fractured basalt rocks. The depth, thickness, and conductivity of each layer were estimated by correlating geotechnical surveys with finite element simulations of the Wenner method. An agreement with measurements was obtained within 10% error margin [19]. Table 1 shows the final values of the soil conductivities for all LST sites.

2.3. Foundation and Baseline Design of the Earthing System
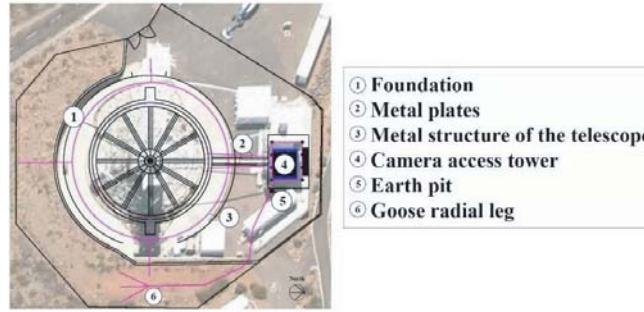
The foundations of the telescopes are made of concrete and a steel bar armature. They have a central part of reinforced concrete under the axis of rotation of the telescope. A circular beam of reinforced

Table 1. Soil resistivity and geometrical parameters of the soil considered in models for LST telescopes.

	Layer depth (m)	σ (S/m)		Layer depth (m)	σ (S/m)
LST1	0–∞	$6.67\ 10^{-4}$	**LST2**	0–∞	$1.95\ 10^{-4}$
LST3	0–2.85	$0.54\ 10^{-4}$			
	2.85–4.75	$2.86\ 10^{-4}$	**LST4**	0–∞	$4.08\ 10^{-4}$
	4.75–6.25	$0.65\ 10^{-4}$			
	6.25–∞	$6.67\ 10^{-4}$			

concrete is under the rail, and it is connected to the central part with radial beams. Another nearby reinforced concrete foundation is under the camera access tower [20], which is a metallic tower specially designed for two purposes: facilitate the camera maintenance and improve the anchorage of the telescope during storms. In terms of safety, the LST structure has to be equipotential [3, 4, 21].

The design of the LST1 earthing system with the sketch of the metal plate structure is illustrated in Figure 2.

Figure 2. Schematic of the real earthing system designed for LST telescopes. Magenta lines indicate the structure of the horizontal plates used for earthing.

The steel armature of the foundation is connected with metal plates, which are extended outside the reinforced concrete in the four cardinal directions. The metal plates are also connected to the metal structure of the telescope. Lightning rods are integrated in the LST1 structure and the upper level of the camera access tower. They are connected to the earthing system by stainless steel cables which merge in an earth pit with a lightning counter. From this pit, an extension of the earth system was made with a copper plate ended in three additional plates arranged as a goose radial leg and located in the eastern side of the telescope. This installation is done according to UNE standard [22].

3. FINITE ELEMENT SIMULATION

Finite Element Method (FEM) has been used to calculate the earth resistance of the telescopes under test: LST1 and LST3. LST2 and LST4 sites feature a uniform resistivity soil, like LST1. Therefore, as all telescopes are identical the results for LST1 can be rescaled with the resistivities to obtain the expected earth resistances of LST2 and LST4 without additional simulations. FEM simulations were done with COMSOL Multiphysics v5.3a software. For the models presented in this work, Electric Currents Module and a stationary study have been used.

The computational domain is a 3D hemisphere that contains the complete geometry modeled for the earthing system of the telescopes. Soil below earth resistance installation is designed with the characteristics displayed in Table 1. Thus, an homogeneous terrain is considered in LST1 case and a four layer model in LST3, as can be seen in the illustrations of Figure 3.
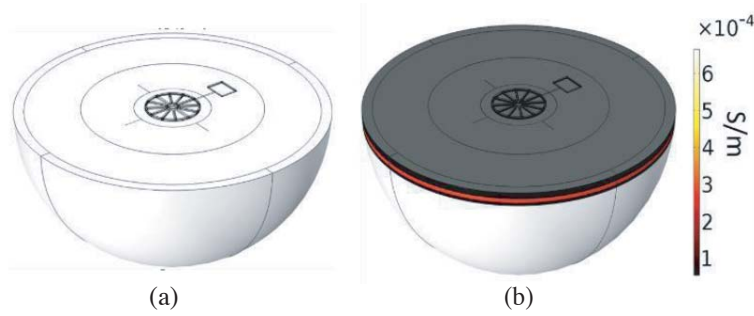
Figure 3. Implemented model geometry and conductivity parameters of the soil. (a) LST1 and (b) LST3.

The earthing system modeled, based on the real one, has two main parts:

- The metal grid. This consists of two solid blocks. One of them is located under the telescope camera and the other under the mirror.
- A composition of thin metal plates. They are surrounding and connected to the solid blocks.

As a guide to consider the size of the structure, one can take as a reference that the distance between the centers of the two solid blocks is 28.5 m. An illustration of the complete interconnected electrodes in COMSOL and a representative simulation scenario is shown in Figure 4. To avoid contour artifacts due the finiteness of the simulated volume, an *Infinite Element Domain condition* has been imposed to an external layer. Electrical ground ($V = 0$) is located at the infinite. A hemisphere surrounding the earthing system limits the zone of interest, where a more dense mesh is made.
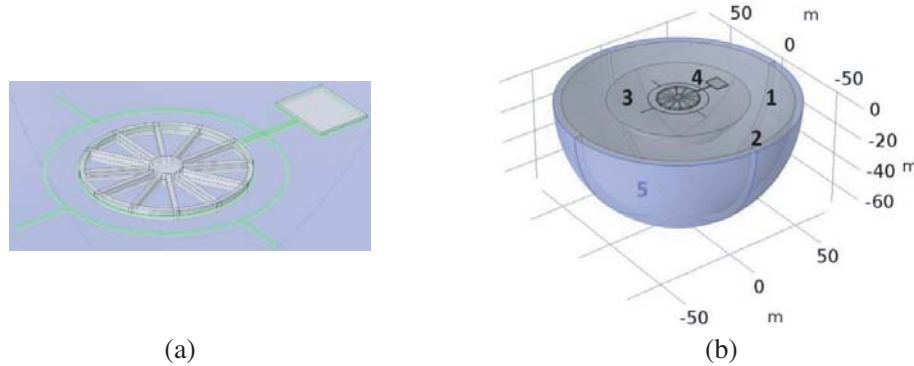

Figure 4. (a) Basic structure designed in COMSOL for the earthing system of the telescopes. (b) Metal grid of the reinforce is displayed in grey color and metal plates surrounding it are in green. Implemented model geometry. (1) Soil (LST1 case). (2) Infinite Element Domain Layer. (3) *Extra fine* mesh zone surrounding earth resistance structure. (4) Earth resistance structure. (5) Ground.

According to the materials used in the LST1 earthing system, metal plates are designed with 3.5 mm height and 30 mm width. Material for the electrodes (solid blocks and plates) has the properties of structural steel ($\sigma = 4.032\ 10^6$ S/m, according to COMSOL's Materials Library).

For boundary condition, the complete earth resistance structure is considered as current source of 1 A. Then, applying Ohm's equation, COMSOL calculates the resistance of the terminal and voltage distribution.
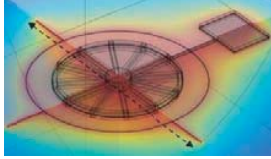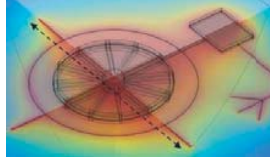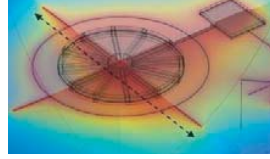
The main difficulty of these simulations comes from the high difference among the relevant dimensions involved in the geometry of the models (lengths in the order of mm combined with others with several m). To avoid that the mesh is too coarse or contains adjacent elements with large differences in scale, the meshing should be made with a nonuniform density. An *Extremely fine* condition set
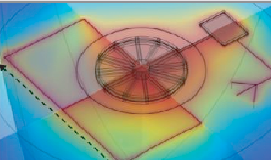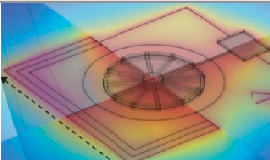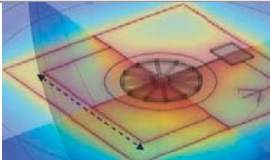
by COMSOL was chosen for the thin plates, an *Extra fine* condition for the solid blocks and the surrounding soil (zone 3 in Figure 4). Finally, the other domains are meshed with *Normal* condition. Additionally, the external layer of the hemisphere has a special distribution appropriated for contour domains called *Boundary Layers.* Despite this differentiation, it was necessary to adjust the tetrahedral element minimum size because some domains are too narrow with respect to the rest of the geometry, and very short boundary segments were necessary. On average, a quality factor of 0.5 is achieved in all models.

4. RESULTS AND DISCUSSION

The optimization of the earthing system in each telescope has been studied. We evaluate the impact in the earth resistance value of several structural modifications with respect to the baseline configuration. Tables 2 and 3 show the results for LST1 and LST3, respectively. Normalized voltage distribution in 3D, calculated earthing system resistance R_{ES}, and percentage of R_{ES} reduction with respect to the original (improvement) are all shown in the tables. As a reference to better visualize the dimensions, a dotted line corresponding to 53.5 m length is also included in the images.
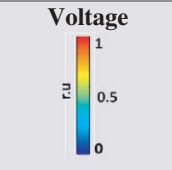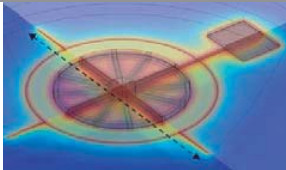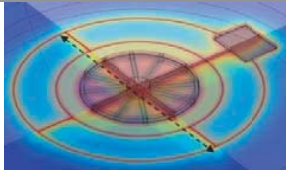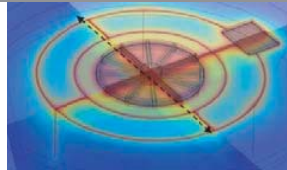
Table 2. Comparison among the models to lower the earth resistance in LST1 telescope. Dashed line corresponds to a 53.5 m length. The voltage shown is normalised to the peak one.

Structure	1.1	1.2	1.3
Voltage			
Modification	Baseline (original)	Add a radial leg metal plate	Add two vertical rods of 10 m in the radial leg
R_{ES} (Ω)	15.17	13.91	13.27
Improvement	-	8.3%	12.5%

Structure	1.4	1.5	1.6
Voltage			
Modification	Surrounded with an external plate	Surrounded with 3 external plates	Surrounded with 3 external plates (bigger)
R_{ES} (Ω)	11.01	9.82	7.14
Improvement	27.4%	35.3%	52.9%

It can be seen that for some configurations, the observed resistance is very high as compared to the widely accepted 10 Ω limit for structures with a lightning protection system. In the case of LST3 telescope, the soil immediately surrounding the earth electrodes has a high resistivity value. The intent is to reduce the earth electrode resistivity using the possibilities that have been presented in this work (adding metal plates of different shapes). Based on the results obtained, there is a need to discuss the applicability of different modifications depending on the case under study.

Table 3. Comparison among the models to lower the earth resistance in LST3 telescope. Dashed line corresponds to a 53.5 m length. The voltage shown is normalised to the peak one.
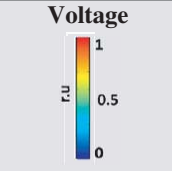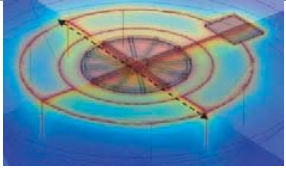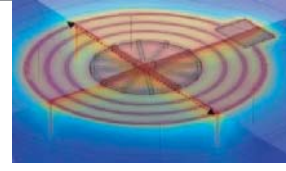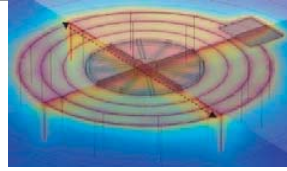
Structure	2.1	2.2	2.3
Voltage			
Modification	Basic (original)	Surrounded with an external plate	Surrounded with an external plate with 3 vertical rods
R_{ES} (Ω)	69.23	53.46	37.87
Improvement	-	22.8%	45.3%

Structure	2.4	2.5	2.6
Voltage			
Modification	Surrounded with an external plate with 7 vertical rods	Surrounded with an external plate with 7 vertical rods and plates of 60 cm (x20)	Surrounded with an external plate with 22 vertical rods
R_{ES} (Ω)	27.90	25.51	23.58
Improvement	59.7%	63.1%	64.2%

4.1. Systems with Horizontal Plates

When the earth resistance is not low enough, lengthening the horizontal earth electrodes in the soil is a popular solution [23]. The comparison of 1.4 with 1.6 indeed reveals the effectivity of extending the plates away from the main structure, to favor the dissipation of the electric current in a larger surface. When all plates are located too close from each other, the decrease of the resistance is marginal. This can be illustrated by comparing 1.5 configuration with 1.4. Despite the addition of two external plates, the improvement is only 7.9%. This result agrees well with previous works which show that resistance in designs with higher density of rods in the center of the grounding grid is often higher than those designs that place the rods at the grid periphery [24]. This is attributed to the shielding effect between electrodes.

The use of radial plates usually improves the resistance of the earthing system, by allowing current to diverge on each conductor, offering lower impedance [25]. This technique seems more effective than a single long conductor. It is also recommended to install at least one vertical electrode per radial conductor when it can connect to a lower resistivity soil layer [26]. In our case, both scenarios 1.2 and 1.3 consider this case. The radial "goose leg" added in 1.2 has a resistance of 54.24 Ω as calculated with COMSOL. Since this value is high as compared to the 15.17 Ω of the main structure, it does not contribute that much to the decrease. For this reason, adding vertical electrodes in this part of the structure is not the optimal solution in terms of improvement (4.2%) and cost.

The discussion for nonuniform soils is more complex. The difference of current distributions in the layers rises when reflective coefficient increases due the resistivity value change in the interfaces. In our case, we have a high resistivity upper layer. It seems that lower earth resistance can be obtained through matching deep low resistivity materials, i.e., with vertical electrodes. If we compare 2.1 and 2.2 cases, a significant improvement is achieved (22.8%), but installing additional and/or wider horizontal plates (case 2.5) does not result into a noticeable effect as compared to previous models. The high

resistivity of the terrain heavily influences the resistance of the structure and imposes a limit to the current dissipation in this first layer. In this case, connecting electrodes with the best conductive layers is the most effective strategy.

4.2. Systems with Horizontal Plates Combined with Vertical Electrodes

The periphery of the earth system is the best place to insert vertical electrodes [27]; therefore, this was the place chosen for the simulation trials. In LST1, structure 1.3 did not show a noticeable improvement with 10 m long metal plates in the end of the radial leg. To evaluate how effective is for this case to bury vertical electrodes in the earthing system, we studied the effect of adding to structure 1.6 plates of 10 m. We added 2, 4, 6 (structure 1.7), 8 10, 12 (structure 1.8) and 16 electrodes. Results and representative illustrations are shown in Figure 5.
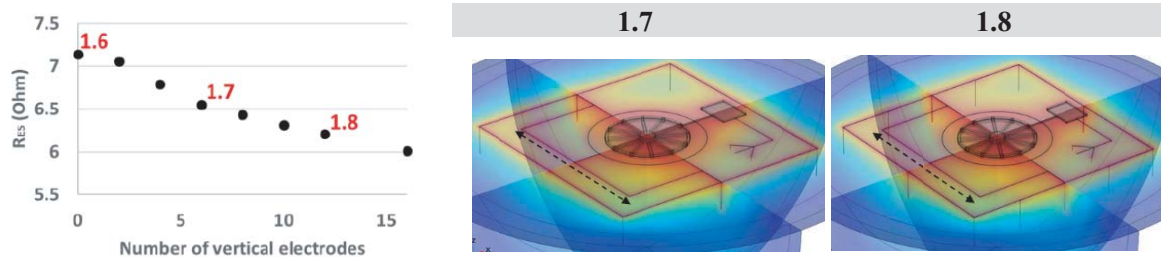

Figure 5. Relationship between the number of vertical electrodes added to structure 1.6 and the calculated earth resistance R_{ES}. Illustration of the cases with 6 vertical electrodes (1.7) and 12 (1.8).

We can confirm that resistance decreases with the increase of the number of vertical electrodes. However, the tendency shows that a saturation is expected when the number of electrodes is very high, because the shielding effect increases [27, 28].

On a multilayered soil, the method of long vertical electrodes does not improve the situation when the soil resistivity of the bottom layer is very high. On the other hand, when a low resistivity soil layer is under a higher one, adding deep electrodes can achieve good results. The comparison of 2.2 with 2.3 and 2.4 shows that long vertical electrodes can always reach better results. However, in 2.6 we have increased the number of vertical electrodes up to 22, and the enhancement is not as noticeable as desired. This could be related with the current reflections produced due to resistivity interfaces. So, the choice of electrode length, location, and number is determined by the soil structure.

4.3. Simulations of Parallel Connection of Earthing Systems

The large resistivity of the LST3 site is the main factor limiting the earth resistance minimization for this telescope. However, the fact that the four LSTs are far enough from each other offers the possibility of efficiently reducing the earth resistance by interconnecting all the earth layouts, which in practice means a connection of four resistors in parallel. According to previous work on the behavior of vertical electrodes connected in parallel, the electrodes must be separated from each other at least five times of their equivalent radius, so the ground potential has decayed to 20% of the potential rise [29]. However, this result cannot be applied in a straightforward way to the connection of the LST earth systems for two main reasons: the optimum layouts for uniform terrains are very shallow, and it is unclear what would be the influence of the non-uniformity of the LST3 soil resistivity.

In order to clarify these points a simulation was done by considering a structure in which LST1 and LST3 earth systems are connected, taking into account the different soil resistivities under them. Figure 6 shows a schematic of the model geometry.

The calculations using FEM are presented in Table 4. In the first column, the case in which both structures are present but not inter-connected is shown. In the second column, we connect them with an horizontal steel plate similar to the one used in the previous designs. The current source for the
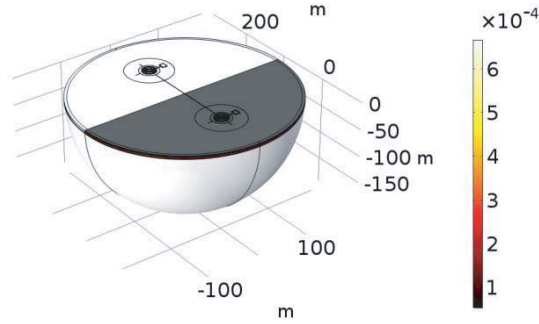
Figure 6. Implemented model geometry and conductivity parameters of the soil for the case in which LST1 ans LST3 are interconnected.

Table 4. Comparison among the results for LST3 earth resistance value (R_{ES}) when LST1 and LST3 structures are present and they are/not interconnected in parallel. The current terminal condition is imposed in LST3 (represented in color blue).

Structure	Separated	Parallel
Description		
	Ground-structures independent	Ground-structures connected in parallel
Voltage		
R_{ES} (Ω)	70.74	11.6
Improvement	-	**82.7%**

earth resistance calculation is injected at the LST3 earth system. Voltage distribution, equipotential curves, and earth resistances are shown in the table.

Since LST1 resistance is $15.17\,\Omega$ (see structure 1.1 in Table 2), the rule for two resistances in parallel predicts a $12.5\,\Omega$ resistance value for this configuration. The reduction needed to accomplish the requirements is almost achieved with a reduction of 82.7% of the resistance of LST3 earth. Furthermore, the simulation shows that the inter-telescope distances are long enough, and the non-uniformity of LST3 soil does not make any strong influence on the accuracy of the simple parallel resistor model. Assuming linearity between the soil resistivity and earth resistance for the homogeneous soils and making use of the fact that all telescopes are identical, it is possible to estimate the earth resistances for LST2 and LST4 without further simulations, and calling ρ_i to LST_i soil resistivity we can estimate the earth resistances R_{ES_i} as

$$R_{ES_i} = \rho_i \frac{R_{ES_1}}{\rho_1} \tag{1}$$

Using expression (1) one readily obtains that the total earth resistance for the complete LST subarray would be $7.2\,\Omega$.

5. CONCLUSIONS

Different methods of lowering the earth resistance value modifying the earthing structure design and calculating its value with Finite Element simulation have been discussed in this paper. The results demonstrate how the voltage distribution and earth resistance value are influenced by the earthing system design. To evaluate the optimum modifications that should be made, we have considered the influence of the shape, size, and number of horizontal and vertical electrodes depending on the soil properties. The possibility of inter-connecting in parallel several structures has also been analyzed.

The following conclusions can be drawn from the simulations described below:

- The optimum strategy for a uniform, high resistivity soil is extending the horizontal plates as far as possible from the main structure. Vertical electrodes do not provide significant improvements.
- If the soil contains several layers vertical electrodes connecting with the best conductivity layer are effective in producing significant resistance reduction.
- It is confirmed by simulations that the interconnection of several earth systems located at distances of the order of five times or more the size of the earth system leads to an arrangement of parallel resistors that can produce considerable earth resistance reductions. This approach is particularly powerful when the installation consists of several facilities built on soils of highly different resistivities. In this case, each facility takes benefit of the best one.

ACKNOWLEDGMENT

REFERENCES

1. International Electrotechnical Commission (IEC), "Protection against lightning — Part 1: General principles," IEC 62305-1, Ed 2.0 2010-12, 2010, https://webstore.iec.ch/preview/info_iec62305-1%7Bed2.0%7Den.pdf.

2. International Electrotechnical Commission (IEC), "Protection against lightning — Part 2: Risk management," 2010, https://webstore.iec.ch/preview/info_iec62305-2%7Bed2.0%7Den.pdf.

3. International Electrotecnical Commission, "Protection against lightning — Part 3: Physical damage to structures and life hazard, IEC 62305-3," 2010, https://webstore.iec.ch/publication/6795.

4. International Electrotecnical Commission, "Protection against lightning — Part 4: Electrical and electronic systems within structures, IEC 62305-4," 2010, https://webstore.iec.ch/searchform&q=IEC 62305-4.

5. "ITC-BT-18," Ministerio de Ciencia y Tecnologia, 2018.

6. Ueng, T. T.-S., Y.-C. Lin, J.-C. Chang, and C.-K. Kuan, "The ground testing of tps ground system," 2011, https://accelconf.web.cern.ch/ipac2011/papers/tups062.pdf (accessed: Jun. 06, 2020).

7. British Standards Institution, "Code of practice for protective earthing of electrical installations BS 7430:2011," No. 1, 1–96, 2011, https://global.ihs.com/doc_detail.cfm?document_name=BS 7430&item_s_key=00131083&csf=TIA (accessed: Jun. 06, 2020).

8. "Military handbook grounding, bonding and shielding for electronic equipments and facilities Volume I of II Volumes basic Theory," 1982, https://www.wbdg.org/FFC/NAVFAC/DMMHNAV/hdbk419a_vol1.pdf (accessed: Jun. 06, 2020).

9. Electric Engineer Portal, "Measurements and calculations of Earth electrode systems," https://electrical-engineering-portal.com/earth-electrode-systems#types-earth-electrodes (accessed: Jun. 06, 2020).

10. IEEE Std 80, *Guide for Safety In AC Substation Grounding*, Vol. 2000, Feb. 2000.

11. Okyere, P. Y. and G. Eduful, "Reducing Earth electrode resistance by replacing soil in critical resistance area," *J. Mod. Eng.*, 2006, doi: 10.4314/just.v29i2.46230.

12. "IEC 62561-7:2018 Lightning protection system components (LPSC) — Part 7: Requirements for earthing enhancing compound," *International Standard*, 2018, https://webstore.iec.ch/publication/33885 (accessed: Jun. 06, 2020).

13. Lindsay, T., "National electrical grounding research project, technical report," 2007, https://www.nfpa.org/-/media/Files/News-and-Research/Archived-reports/negrpfinalreport.ashx?la=en.

14. "LST — Cherenkov telescope array," https://www.cta-observatory.org/project/technology/lst/ (accessed: Jun. 15, 2020).

15. Cortina, J. and M. Teshima, "Status of the Cherenkov telescope array's large size telescopes," 2015, http://cta-observatory.org (accessed: Jun. 15, 2020).

16. Sabiha, N. A. and N. I. Elkalashy, "Evaluation of grounding system design for wind farm using COMSOL," 2018, http://www.ripublication.com (accessed: Jun. 26, 2020).

17. Malanda, S. C., I. E. Davidson, E. Singh, and E. Buraimoh, "Analysis of soil resistivity and its impact on grounding systems design," *2018 IEEE PES/IAS PowerAfrica, PowerAfrica 2018*, 324–329, Nov. 2018, doi: 10.1109/PowerAfrica.2018.8520960.

18. Wenner, F., "A Method of measuring Earth resistivity," *Bull. Bur. Stand.*, Vol. 12, 469–478, 1916, doi: https://doi.org/10.6028/bulletin.282.

19. Ronda, S., O. Martinez, C. Oliver, P. Marquez, and J. M. Miranda, "Finite element analysis and experimental characterization of soil electrical resistivity at El roque de los muchachos observatory," *Journal of Electromagnetic Analysis and Applications*, Vol. 12, No. 7, 89–102, 2020.

20. De A. de Canarias, I., "LIC-15-034: Construction of foundation of Telescope LST1," 10, Plataforma de Contratación del Estado (Spain), 2015, https://contrataciondelestado.es/wps/wcm/connect/8e64f971-f3eb-41d1-a206-edca7ec9b590/DOC_CD2015-229760.pdf?MOD=AJPERES (accessed: Jun. 15, 2020).

21. Ma, J., T. Del Pino, and S. P. Martí, "NTP-1.084: Prevención de riesgos laborales originados por la caída de rayos," 2017.

22. "UNE 21186:2011 Protección contra el rayo: Pararrayos con dispo," 2011, https://www.aenor.com/normas-y-libros/buscador-de-normas/une/?Tipo=N&c=N0048559 (accessed: Jun. 25, 2020).

23. El-Sayed Gouda, O., *Design Parameters of Electrical Network Grounding Systems*, IGI Global, 2018.

24. Zeng, R., J. He, Z. Wang, Y. Gao, W. Sun, and Q. Su, "Analysis on influence of long vertical grounding electrodes on grounding system for substation," *PowerCon 2000 — 2000 International Conference on Power System Technology, Proceedings*, Vol. 3, 1475–1480, 2000, doi: 10.1109/ICPST.2000.898188.

25. El-Sayed Gouda, O., *Design Parameters of Electrical Network Grounding Systems*, IGI Global, 2018.

26. Lim, S. C., C. Gomes, and M. Z. A. Ab Kadir, "Electrical earthing in troubled environment," *Int. J. Electr. Power Energy Syst.*, Vol. 47, No. 1, 117–128, May 2013, doi: 10.1016/j.ijepes.2012.10.058.

27. Zeng, R., J. He, Z. Wang, Y. Gao, W. Sun, and Q. Su, "Analysis on influence of long vertical grounding electrodes on grounding system for substation," *PowerCon 2000 — 2000 International Conference on Power System Technology, Proceedings*, Vol. 3, 1475–1480, 2000, doi: 10.1109/ICPST.2000.898188.

28. Malanda, S. C., I. E. Davidson, E. Singh, and E. Buraimoh, "Analysis of soil resistivity and its impact on grounding systems design," *2018 IEEE PES/IAS PowerAfrica, PowerAfrica 2018*, 324–329, Nov. 2018, doi: 10.1109/PowerAfrica.2018.8520960.

29. Mitolo, M., *Analysis of Grounding and Bounding Systems*, CRC Press, 2020.